

Design of Reconfigurable Monopole Antenna with Switchable Dual Band-Notches for UWB Applications

Ji Li and Yufa Sun*

Abstract—A reconfigurable antenna with on-demand single-band or dual-band rejection capability for ultra-wideband (UWB) applications is presented. A modified monopole structure is integrated with a U-shaped slot and an open-ended slot to realize band-rejection. The antenna operates in four modes: a full UWB (3.1–10.6 GHz) coverage antenna, a UWB antenna with a single-band WiMax or wide local area network (WLAN) rejection, and a UWB antenna with dual-band WiMax/WLAN rejection. On-demand single and dual-band rejections are implemented by controlling two slots using two PIN diodes. Thus, the adopted control technique is quite easy and requires low operating power. Details of the design process and reconfiguration mechanism are presented. The band-rejection performance is explained by return loss and surface current distribution at single-band mode. A prototype is built on a Rogers substrate and tested to validate the performances. The antenna exhibits stable radiation characteristics and almost flat gain responses across the whole band, while significantly gain reduction is achieved at the rejected bands. Therefore, this antenna is suitable for high-performance UWB systems in WiMax/WLAN dense environments with the aim to improve signal quality, system capacity, and communication efficiency.

1. INTRODUCTION

In the last few years, ultra-wideband (UWB) technology operating across the band 3.1–10.6 GHz has received fascinating attention due to its merits, such as low-power requirement, large channel capacity, and resistance to jamming [1, 2]. Owing to these advantages, UWB technology has been adopted widely in many fields such as short-range indoor communications, imaging systems, radar and target localization, and automotive applications [3–5]. Therefore, UWB antenna is well researched, and many low-profile printed antennas have been proposed [4–8]. There are several narrow band standards that coexist within the UWB, of which the commonly used bands are IEEE 802.16 WiMax (3.3–3.6 GHz, 5.25–5.825 GHz), IEEE 802.11a wide local area network (WLAN) (5.15–5.35 GHz, 5.725–5.825 GHz), and ETSI HiperLAN/2 (5.15–5.35 GHz, 5.47–5.725 GHz). The overlap of bands causes electromagnetic interference when a number of devices run simultaneously at these bands [9–13]. In such a case, in-band interference occurs between the narrow band communication device with strong signal transmission and the UWB system, and the UWB system may also interfere with those narrow band devices that receive a weak signal. In this regard, many UWB antennas with inherent band-rejection properties have been investigated using different techniques [14, 15]. However, band-rejection is not constantly required, but on-demand band-rejection is more desirable. Thus, adapting reconfigurable band-rejection technique with UWB antenna is an effective way to satisfy on-demand band-rejection requirements [9, 10, 12, 16].

Recently, several UWB antennas with reconfigurable band-rejection capability using active switching elements such as PIN diodes [17, 18], varactors [19], radio frequency (RF) microelectromechanical

Received 14 August 2019, Accepted 17 September 2019, Scheduled 29 September 2019

* Corresponding author: Yufa Sun (yfsun_ahu@sina.com).

The authors are with the Key Lab of Intelligent Computing and Signal Processing, Ministry of Education, Anhui University, Hefei 230601, China.

systems (MEMS) [13] and optically controlled switches [20, 21] have been reported. Different types of switches can be used in different types of antenna designs [22–24]. Most of these antennas are capable of rejecting or tuning a single band only (WiMax or WLAN separately). UWB antennas with multiple rejection modes are also reported, but they do not support the full UWB (no rejection) mode. Therefore, to be fully compatible with planar UWB systems, besides the simple construction and easy control, UWB antenna must possess reconfigurable rejection ability to reject single, dual band (WiMax/WLAN) or none, as required by the user.

In this paper, a planar, simple construct and easy to control UWB antenna with on-demand rejection capability is proposed. The antenna can work in UWB, single band-rejection (WiMax or WLAN), and dual band-rejection (WiMax and WLAN) modes. The proposed antenna incorporates a U-shaped slot in the feedline of a monopole and an open-end slot near the upper edge of the radiator. Four reconfigurable modes are realized by using two PIN diodes. Thus, it requires low operating power. The design details, performances analysis, and measured results are presented as follows. In addition, the antenna performances are compared with some recently reported works to present its added flexibility and distinctive reconfigurable features using a simple control technique.

2. ANTENNA DESCRIPTIONS

2.1. Antenna Structure

Based on the aforementioned introduction, the design procedure of the proposed antenna can be presented as the following figures. The basic antenna structure is composed of a rectangular patch fed by a microstrip line and a ground plane. The substrate is Rogers RT/duroid5880 (dielectric constant $\varepsilon_r = 2.2$, height $h = 0.787$ mm, and loss tangent = 0.0009). The fundamental resonant frequency of a printed antenna with ground plane can be approximated by the formula given in [25]:

$$f_r = \frac{144}{L_g + L_r + g + (A_g/2\pi L_g \sqrt{\varepsilon_e}) + (A_r/2\pi L_r \sqrt{\varepsilon_e})} \quad (1)$$

Here, L_g and L_r are the lengths of the ground plane and radiator, respectively; g is the gap between them; A_g and A_r are the areas of the ground plane and radiator, respectively; and the effective dielectric constant is $\varepsilon_e = (\varepsilon_r + 1)/2$, where ε_r is the dielectric constant of the substrate. The basic structure of microstrip antenna does not have a desirable frequency response in UWB. However, according to Figure 1, the initial structure of the antenna is transformed to improve the frequency response, and their return losses (S_{11}) for different antennas are plotted in Figure 2.

The proposed design gradually evolves from Antenna 1 to Antenna 6 as shown in Figure 1. For the lowest resonance, the lengths of the radiator ($L_r \approx L_s$) should be approximately $\lambda_e/4$, where λ_e is the effective wavelength at the target frequency. With these preliminary assumptions, the UWB antenna design is initiated from Antenna 1, while using Equation (1) to estimate its fundamental resonance. The design parameters of the antenna are shown in Table 1.

Table 1. Dimensions of the proposed antenna.

Parameters	L	L_f	L_g	L_s	L_t	L_v
Value/mm	35 (0.41 λ_0)	16.8 (0.20 λ_0)	16.4 (0.19 λ_0)	17 (0.20 λ_0)	14.7 (0.17 λ_0)	4.6 (0.05 λ_0)
Parameters	L_u	L_w	L_e	L_a	W	W_u
Value/mm	3.1 (0.04 λ_0)	10.9 (0.13 λ_0)	10.4 (0.12 λ_0)	12.3 (0.14 λ_0)	25 (0.29 λ_0)	1.5 (0.02 λ_0)
Parameters	W_g	W_{gg}	W_f	W_s	R_1	R_2
Value/mm	0.3 (0.004 λ_0)	1.2 (0.01 λ_0)	2.5 (0.03 λ_0)	18 (0.21 λ_0)	7.4 (0.09 λ_0)	2.5 (0.03 λ_0)

λ_0 is the wavelength of the center frequency of the first band notch.

Antenna 2 is formed by inserting a rectangular slot in the middle of the ground plane of Antenna 1. As shown in Figure 2, Antenna 2 has good impedance matching in the wide band of 3.6–14 GHz,

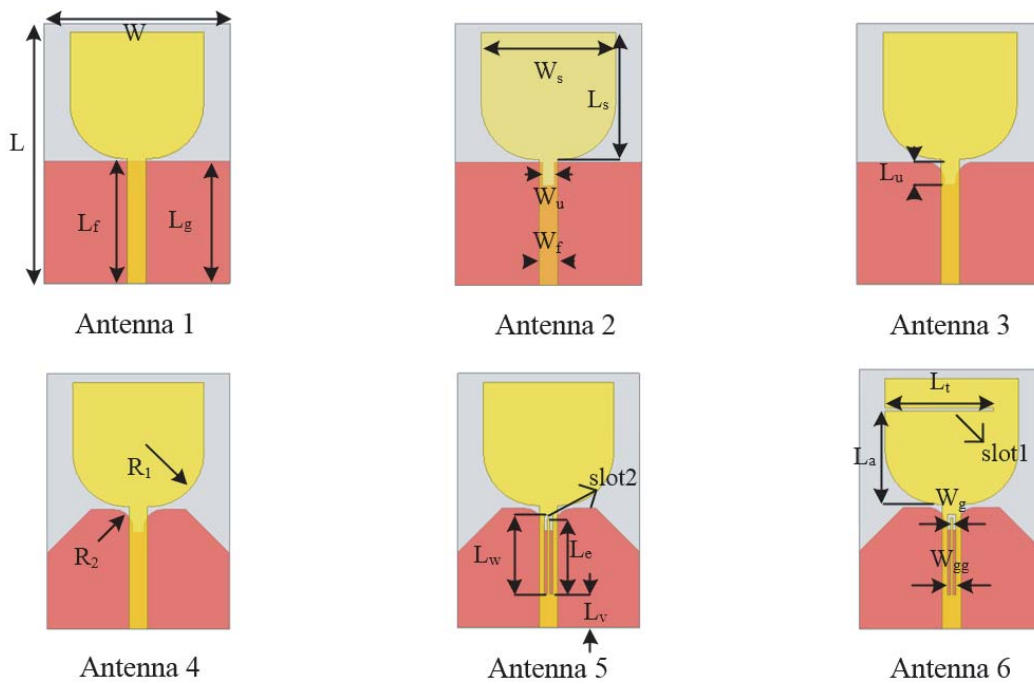


Figure 1. Evolution of the proposed antenna.

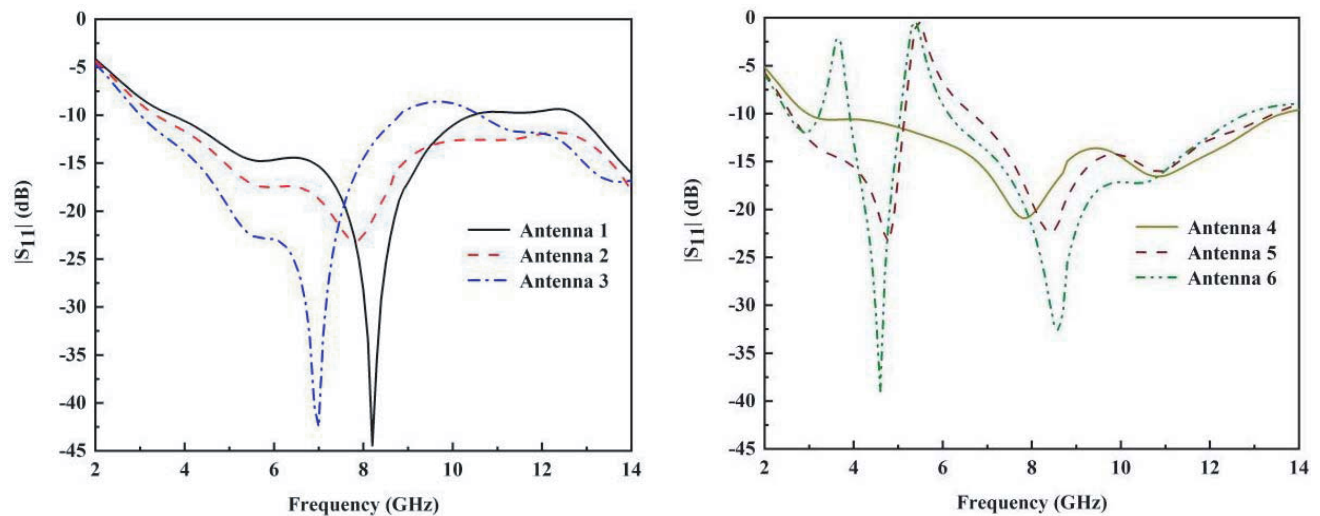


Figure 2. Return loss $|S_{11}|$ of various antenna structures.

but it still cannot completely cover the low frequency of UWB. Thus, Antenna 2 is further improved with arc-slits to form Antenna 3. It can be seen from Figure 2 that Antenna 3 has better impedance matching than Antenna 2 at low frequency, but the high frequency impedance matching is deteriorated. In order to improve the high frequency impedance matching, two chamfers are added on the ground plane of Antenna 3 to form Antenna 4. As shown in Figure 2, Antenna 4 covers a very wide band (3–13.8 GHz) and matches well ($S_{11} \leq -10$) within the UWB. By adding resonant structures, Antenna 5 and Antenna 6 generate notched bands in the frequency response of WLAN and WiMax/WLAN, respectively.

2.2. Design of the Reconfigurability and Simulated Performances of the Antenna

After designing the well-matched UWB antenna (Antenna 4), band-rejection function is realized by utilizing an open-ended slot (slot1) and a U-shaped slot (slot2) in Antenna 6. The rejected resonances f_{r1} and f_{r2} are controlled by adjusting the lengths of slots (L_{slot1} and L_{slot2}). The relations of f_r with L_{slot} are shown in Equation (2) and Equation (3).

$$f_{r1} = \frac{C_0}{4L_{slot1}\epsilon_e}, \quad (2)$$

$$f_{r2} = \frac{C_0}{2L_{slot2}\epsilon_e}, \quad (3)$$

where C_0 is the light speed, and f_{r1} and f_{r2} are the center frequencies of rejected bands, respectively. The two slots affect the surface current distribution on the antenna at the respective frequency, and f_{r1} , f_{r2} can be easily controlled by adjusting L_{slot} . Figure 3 shows the effect of L_{slot} on tuning the rejected band within the UWB range. As the lengths of L_t and L_w become longer, the center frequency of the rejected band shifts toward the low frequency. This is consistent with the result derived from Equation (2) and Equation (3). According to Equation (2), the length of open-ended slot, L_{slot1} (L_t) = 14.7 mm is approximately $\lambda_e/4$ at the WiMax band, thus the antenna rejects this band at 3.6 GHz. Similarly, from Equation (3), the length of U-shaped slot, $L_{slot2} = 2 * L_w + W_g$ is approximately $\lambda_e/2$ at the WLAN band. When $L_w = 10.9$ mm, the antenna rejects this band at 5.5 GHz.

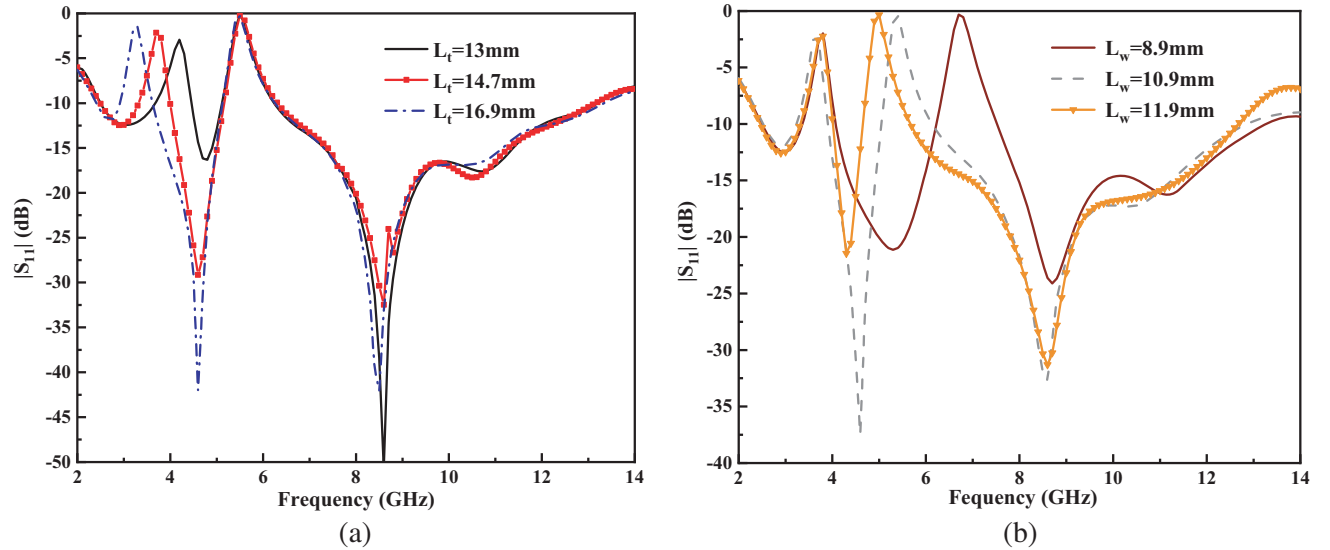


Figure 3. Effect of L_{slot} on return loss of the proposed antenna. (a) Open-ended slot (L_t). (b) U-shaped slot (L_w).

As shown in Figure 4, slot1 is controlled by PIN diode D1, and slot2 is controlled by PIN diode D2. Four reconfigurable modes can be realized from the single antenna. Depending on biasing conditions of D1 and D2, the two slots become active or inactive in playing their band-rejection roles. Thus, the antenna can be switched from a normal UWB to a single or dual band rejection mode. Figure 4(a) depicts the details of the proposed antenna including the biasing circuit. The MA-COM PIN diode MA4AGFCP910, which has a very low capacitance ($C_t = 0.018$ pF) and low resistance ($R_s = 5.2 \Omega$ at 10 mA), is considered for switching purpose. The diode exhibits 2–3 ns switching characteristics, and the ultra low capacitance of the MA4AGFCP910 allows it to use through millimeter frequencies for RF switch applications. Thus, this diode becomes a suitable choice. The ‘ON’ and ‘OFF’ states of the PIN diode and its biasing circuit are given in Figure 4(c). In the biasing circuit, a 28 nH biasing inductor L together with a high impedance biasing line is used for choking RF signal, and a resistor $R = 120$ ohm

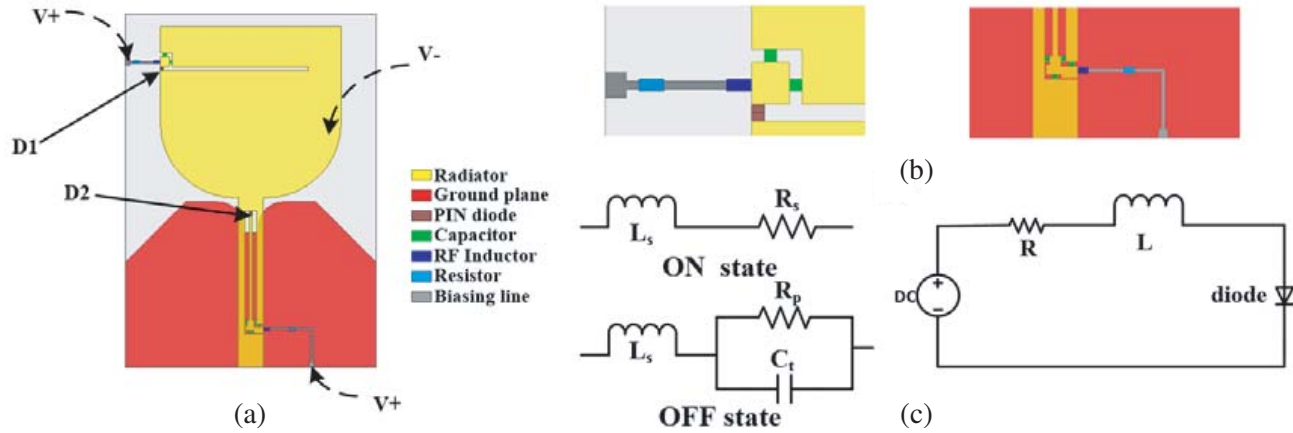


Figure 4. Details of the proposed reconfigurable UWB antenna design. (a) Antenna configuration. (b) Partial view of the DC bias circuit. (c) DC biasing circuit of the PIN diode.

in the biasing line is used for limiting the maximum forward bias current of the diode at the supplied voltage. In addition, a capacitor is used to conduct RF and separate the positive and negative terminals of the direct current (DC) power supply across the diode. Many small rectangular grooves engraved on patch, PIN diode, and its biasing circuits will affect the performance of antenna. To compensate the effects of diode and these slots, slot1 and slot2 are adjusted to maintain $\lambda_e/4$, $\lambda_e/2$ for proper WiMax and WLAN band-rejection.

The simulation and optimization are done in an Ansys HFSS electromagnetic simulator. The $|S_{11}|$ in the four modes of operation is shown in Figure 5. When two diodes are in ON state, antenna radiates in the UWB (Case 1). When D1 is OFF and D2 ON, the UWB operating bandwidth with notch band at WiMax is obtained (Case 2). In Case 3, when D1 is ON and D2 OFF, UWB with notch band at WLAN is achieved. Moreover, when two diodes are OFF, UWB with dual notch band characteristics is achieved (Case 4). The relationship between the switch states and the different modes is shown as Table 2. In addition, the operating bandwidth and rejected bandwidth for each mode can also be seen from Table 2. Therefore, the changes in switching state of PIN diodes provide the reconfigurability among available notch bands in the UWB.

Table 2. Operation conditions of reconfigurable antenna.

	Case 1	Case 2	Case 3	Case 4
D1	ON	OFF	ON	OFF
D2	ON	ON	OFF	OFF
RBW (GHz)	No band rejection	3.1–3.95	4.8–6.15	3.3–3.96 4.7–5.85
OBW (GHz)	2.8–13.8	2.7–13.4	2.6–13.3	2.5–13

RBW, rejected bandwidth; OBW, operating bandwidth.

The principle of the rejection is that the slot excites resonance at the frequency corresponding to its length, such that the current path is blocked and concentrated around the slot. The current distribution on the antenna surface at single-band rejection modes is depicted in Figure 6, which provides a better understanding about the role of the open-ended slot and U-shaped slot in creation of the band notch performance. Figure 6(a) shows the current distribution at the center frequency of the lower band notch (Case 2). It can be seen that the current flow is concentrated around the open-ended slot. At the center frequency of the higher band notch (Case 3), the current distribution which is concentrated around the U-shaped slot is shown in Figure 6(b).

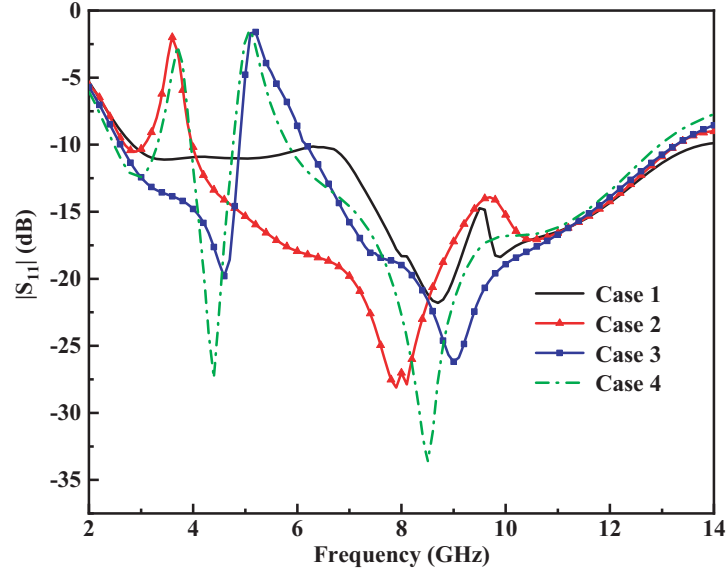


Figure 5. Simulated return loss of the proposed antenna in four operation modes.

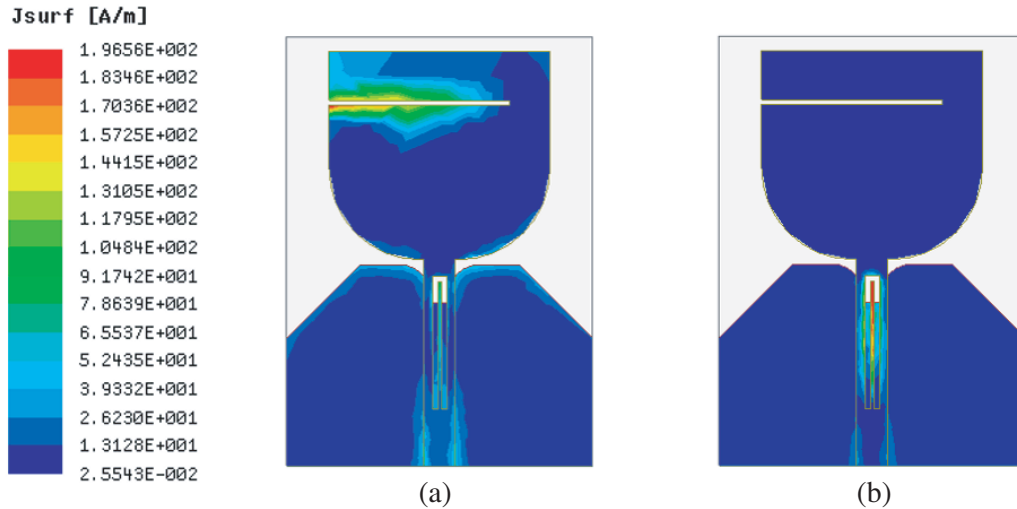


Figure 6. Surface current distributions of the proposed antenna at (a) Case 2, (b) Case 3.

3. MEASURED RESULTS AND DISCUSSION

To verify the proposed design, an antenna prototype is fabricated, as shown in Figure 7. A $50\ \Omega$ sub-miniature A (SMA) connector is used to feed the antenna. A bias DC is provided from the side of the antenna to minimize the effects of the bias circuit on the antenna radiation. Surface mountable chip capacitor ($10\ \text{pF}$) and inductor ($28\ \text{nH}$) from Murata and MA4AGFCP910 PIN diodes are soldered at their predefined positions on the top surface. The simulated and measured return losses for various bias conditions of the PIN diodes are plotted in Figure 8. It can be observed that good agreement exists between the measured and simulated results. However, there are some differences in notch bandwidth due to the fabrication process, implementation of the PIN diodes, and their biasing circuits. The antenna works commonly from $2.8\ \text{GHz}$ to above $13.5\ \text{GHz}$ in all modes. The measured rejected bands are $3.1\text{--}4\ \text{GHz}$ (Case2) with a peak at $3.45\ \text{GHz}$ and $4.95\text{--}6.1\ \text{GHz}$ (Case3) with a peak at $5.3\ \text{GHz}$. When the antenna works in Case4, it rejects the WiMax band ($3.3\text{--}3.96\ \text{GHz}$) centered at $3.6\ \text{GHz}$ and

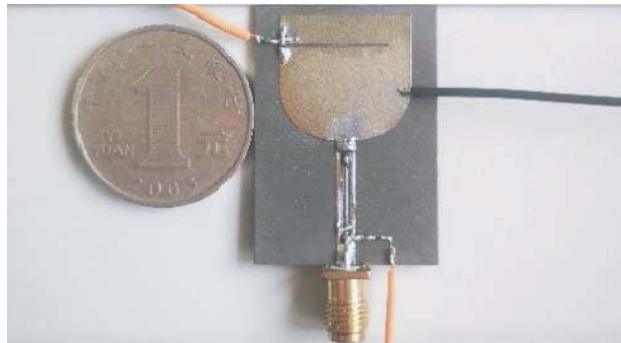


Figure 7. Prototype of the proposed antenna.

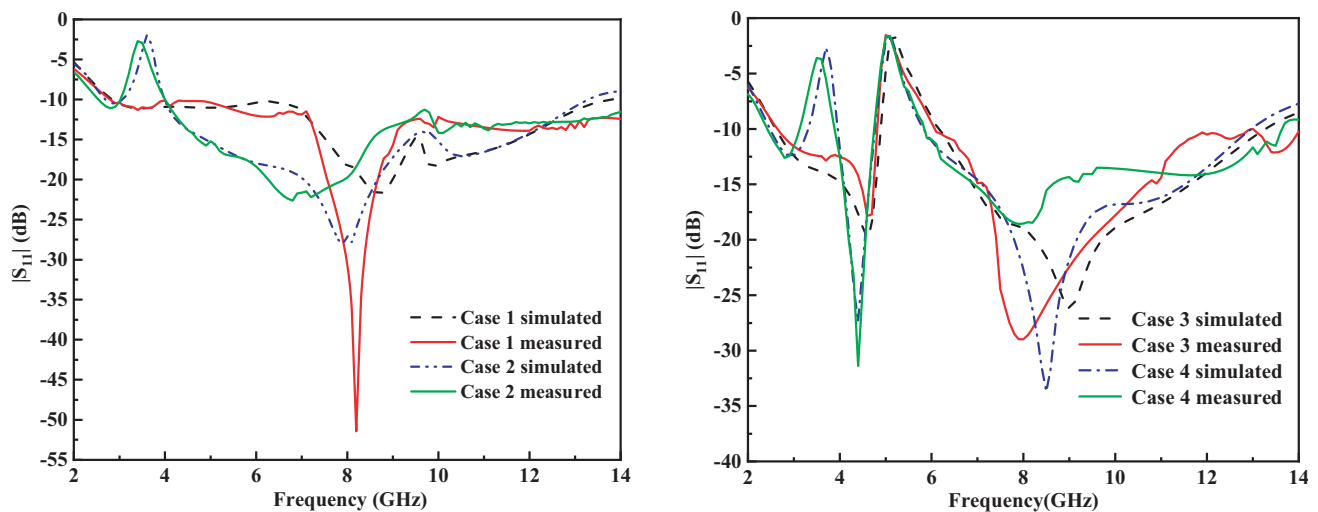


Figure 8. Comparison between simulated and measured return loss of the proposed antenna in four operation modes.

the WLAN band (4.7–5.9 GHz) centered at 5.3 GHz. The measured normalized E -plane (y - z plane) and H -plane (x - z plane) patterns at 4.5, 7, and 9 GHz are shown in Figure 9. The H -plane patterns are almost omnidirectional, which is an advantage for UWB applications. In addition, the measured maximum gain for full UWB coverage and dual band notch performances of the fabricated antenna are compared in Figure 10. It can be seen that the gain drops dramatically at notched frequency bands for Case4. Measured results of $|S_{11}|$, gains, and radiation patterns are obtained by Agilent N5247A network analyzer and a SATIMO antenna measurement system.

The performance and measured results of the proposed antenna are compared with some of the recently reported reconfigurable band-rejection UWB antennas in terms of the size, full UWB coverage, number of PIN diodes, number of reconfigurable operation modes, etc. Detailed comparisons are listed in Table 3. The proposed antenna has reconfigurability between the rejection modes and the normal UWB operation. Although the antenna in [21] has similar functions, the driver arrangement on the antenna requires an extra height, and each switch requires more control power, which increases the cost and limits its application. In comparison, the proposed antenna is controlled by PIN diode and requires less control power, while it still serves the on-demand band-rejection purpose. With this reconfigurability, this antenna adds more freedom to choose the operation mode as required by the UWB system. Thus, it will reduce mutual interference and power loss of the communication systems, and shows potential for many applications.

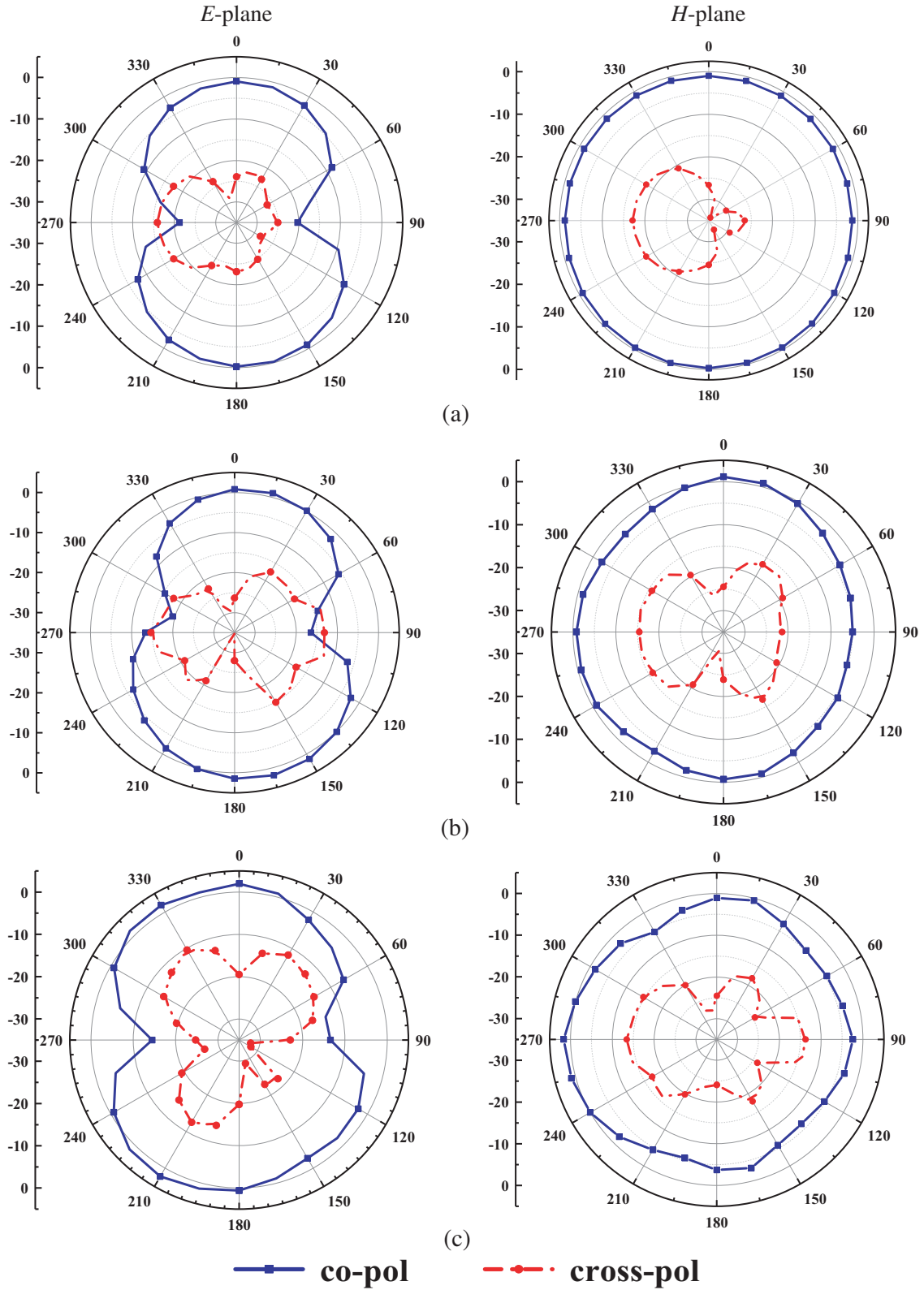


Figure 9. Normalized measured radiation patterns of the proposed antenna at (a) 4.5 GHz, (b) 7 GHz and (c) 9 GHz.

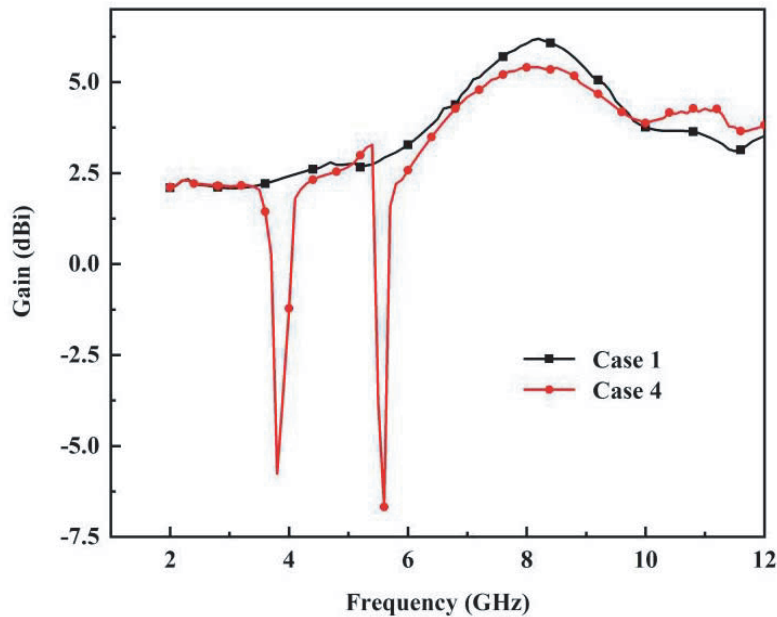


Figure 10. Measured peak gain of the fabricated antenna for Case 1 and Case 4.

Table 3. Comparison with previously published works.

	This work	[7]	[9]	[12]	[18]	[21]
antenna size (mm)	35 × 25 × 0.787	38 × 32 × 1.6	20 × 20 × 0.8	41 × 35 × 1.5	32 × 27	40 × 35 × 1.5
UWB bandwidth, (GHz)	2.8–14	3.05–13	3.1–12.5	2.5–10.8	2.7–10.7	2.6–11
rejected bands, (GHz)	3.1–4 4.95–6.1 3.3–3.96/ 4.7–5.9	3.1–4.05 5.1–6.0 3–3.85/ 5.0–5.95	3.12–3.82 5.0–6.06	3.5 5.5	3.35–3.85 5.05–5.95 3.3–3.8/ 5.1–6.0	3.55 5.08 3.56/5.1
number of PIN diodes	2	3	2	5	3	2
number of operation modes	4	4	3	3	4	4

4. CONCLUSION

In this paper, a UWB antenna with band-stop reconfigurability is proposed. The antenna can work in four modes full UWB, individual WiMax or WLAN rejection, and dual rejection (WiMax and WLAN). An open-ended slot and a U-shaped slot are used to achieve the rejected bands. Reconfigurability is controlled by a low-power control unit consisting of two PIN diodes and a DC bias circuit. For better understanding, the design process and detailed analysis of the reconfiguration mechanism are proposed. Stable radiation characteristics are obtained across the full UWB mode. Gain characteristics are obtained in UWB and dual rejection modes, respectively. When the corresponding rejected band occurs, a significant gain reduction is achieved at the rejected band. With the added flexible rejection capability, avoiding mutual interference between UWB and WiMax/WLAN receivers, the proposed antenna can improve signal quality and communication efficiency.

ACKNOWLEDGMENT

This work is supported by the National Natural Science Foundation of China under Grant 61172020.

REFERENCES

1. Gao, G., B. Hu, and J. Zhang, "Design of a miniaturization printed circular-slot UWB antenna by the half-cutting method," *IEEE Antennas and Wireless Propagation Letters*, Vol. 12, 567–570, 2013.
2. Fontana, R. J., "Recent system applications of short-pulse Ultra-Wideband (UWB) technology," *IEEE Transactions on Microwave Theory and Techniques*, Vol. 52, No. 9, 2087–2104, 2004.
3. Ojaroudi, M. and N. Ojaroudi, "Ultra-wideband small rectangular slot antenna with variable band-stop function," *IEEE Transactions on Antennas and Propagation*, Vol. 62, 490–494, 2014.
4. Ibrahim, A. A., M. A. Abdalla, and A. Boutejdar, "Resonator switching techniques for notched ultra-wideband antenna in wireless applications," *IET Microwaves, Antennas and Propagation*, Vol. 9, 1468–1477, 2015.
5. Tripathi, S., A. Mohan, and S. Yadav, "A compact fractal UWB antenna with reconfigurable band notch functions," *Microwave and Optical Technology Letters*, Vol. 5, 509–514, 2016.
6. Oraizi, H. and N. V. Shahmirzadi, "Frequency- and time-domain analysis of a novel UWB reconfigurable microstrip slot antenna with switchable notched bands," *IET Microwaves Antennas and Propagation*, Vol. 11, 1127–1132, 2017.
7. Alam, M. S. and A. Abbosh, "Reconfigurable band-rejection antenna for ultra-wideband applications," *IET Microwaves, Antennas and Propagation*, Vol. 12, No. 2, 195–202, 2018.
8. Abbosh, A., "Ultra-wideband quasi-yagi antenna using dual-resonant driver and integrated balun of stepped impedance coupled structure," *IEEE Transactions on Antennas and Propagation*, Vol. 61, 3885–3888, 2013.
9. Tasouji, N., J. Nourinia, C. Ghobadi, and F. Tofigh, "A novel printed UWB slot antenna with reconfigurable band-notch characteristics," *IEEE Antennas and Wireless Propagation Letters*, Vol. 12, 922–925, 2013.
10. Aghdam and S. Abazari, "A novel UWB monopole antenna with tunable notched behavior using varactor diode," *IEEE Antennas and Wireless Propagation Letters*, Vol. 13, 1243–1246, 2014.
11. Li, T., H. Zhai, L. Li, C. Liang, and Y. Han, "Compact UWB antenna with tunable band-notched characteristic based on microstrip open-loop resonator," *IEEE Antennas and Wireless Propagation Letters*, Vol. 11, 1584–1587, 2012.
12. Yang, H., X. Xi, H. Hou, Y. Zhao, and Y. Yuan, "Design of reconfigurable monopole antenna with switchable dual band-notches for UWB applications," *International Journal of Microwave and Wireless Technologies*, Vol. 10, 1065–1071, 2018.
13. Nikolaou, S., N. D. Kingsley, G. E. Ponchak, J. Papapolymerou, and M. M. Tentzeris, "UWB elliptical monopoles with a reconfigurable band notch using MEMS switches actuated without bias lines," *IEEE Transactions on Antennas and Propagation*, Vol. 57, 2242–2251, 2009.
14. Xu, J., D. Shen, X. Zhang, and K. Wu, "A compact disc Ultrawideband (UWB) antenna with quintuple band rejections," *IEEE Antennas and Wireless Propagation Letters*, Vol. 11, 1517–1520, 2012.
15. Ojaroudi, S., Y. Ojaroudi, and N. Ojaroudi, "Novel design of reconfigurable microstrip slot antenna with switchable band-notched characteristic," *Microwave and Optical Technology Letters*, Vol. 57, 849–853, 2015.
16. Aboufoul, T. and A. Alomainy, "Reconfiguring UWB monopole antenna for cognitive radio applications using GaAs FET switches," *IEEE Antennas and Wireless Propagation Letters*, Vol. 11, 392–394, 2012.
17. Gao, G., B. Hu, L. He, S. Wang, and C. Yang, "Investigation of a reconfigurable dual notched UWB antenna by conceptual circuit model and time-domain characteristics," *Microwave and Optical Technology Letters*, Vol. 59, 1326–1332, 2017.

18. Srivastava, G., S. Dwari, and B. K. Kanaujia, "A compact UWB antenna with reconfigurable dual notch bands," *Microwave and Optical Technology Letters*, Vol. 57, 2737–2742, 2015.
19. Horestani, A. K., Z. Shaterian, J. Naqui, and F. Martin, "Reconfigurable and tunable s-shaped split-ring resonators and application in band-notched UWB antennas," *IEEE Transactions on Antennas and Propagation*, Vol. 64, 3766–3776, 2016.
20. Liu, X. and M. M. Tentzeris, "Optically controlled reconfigurable band-notched UWB antenna for cognitive radio systems," *Electronics Letters*, Vol. 50, 1502–1504, 2014.
21. Zhao, D., L. Lan, Y. Han, and F. Liang, "Optically controlled reconfigurable band-notched UWB antenna for cognitive radio applications," *IEEE Photonics Technology Letters*, Vol. 26, 2173–2176, 2014.
22. Salim, M. and A. Pourziad, "A novel reconfigurable spiral-shaped monopole antenna for biomedical applications," *Progress In Electromagnetics Research*, Vol. 57, 79–84, 2015.
23. Rajagopalan, H., J. M. Kovitz, and Y. Rahmat-Samii, "MEMS reconfigurable optimized E-shaped patch antenna design for cognitive radio," *IEEE Transactions on Antennas and Propagation*, Vol. 62, 1056–1064, 2014.
24. Row, J. S. and J. F. Tsai, "Frequency reconfigurable microstrip patch antennas with circular polarization," *IEEE Antennas and Wireless Propagation Letters*, Vol. 13, 1112–1115, 2014.
25. Thomas, K. G. and M. Sreenivasan, "A simple ultrawideband planar rectangular printed antenna with band dispensation," *IEEE Transactions on Antennas and Propagation*, Vol. 58, 27–34, 2010.